J. Nig. Ass. Math. Phys.
Vol. 6 (2002)

CALCULATION OF HYPERFINE FIELDS OF 3d AND 4d IMPURITIES IN NICKEL.

J.S. ONONIWU

Department of Physics, Federal University of Technology
P.M.B. 1526 Owerri Imo State Nigeria.

ABSTRACT

Detailed calculations of the electronic, magnetic and hyperfine fields of 3d and 4d impurities in Ni is here presented. We base the calculations on the local spin density approximation of density functional theory and the Korringa – Kohn – Rostoker Greens function method for impurity methods of calculation. The local moments and hyperfine fields of the impurities and their nearest neighbours are self-consistently calculated. We use the formulas derived by Blugel et al 1987 [1] for the proper relativistic generalizations of the contact, orbital and dipolar contributions to the hyperfine field and explicitly calculate relativistic corrections to the contact interaction which are important for 4d impurities. The hyperfine fields can be split up into local and transferred contributions. The later are directly related to the local moments and to the moments of the neighbouring atoms. We report about calculations for dilute alloys using the KKR – Green's function method and for concentrated disordered alloys using the charge-self consistent KKR – CPA method. The values of calculated hyperfine fields are in agreement with the values obtained from experiments.

1. INTRODUCTION

Through hyperfine fields we obtain unique microscopic information about dilute ferromagnetic alloys. The fermi contact – interaction is the dominant contribution to the hyperfine field and is given by the magnetization density at the nucleus of the impurity atom. Experimental information about hyperfine fields of impurities in Fe, Co, Ni and Gd abound and can be found in the data collections of Rao [2] and Krane [3]. It is only recently that theoretical understanding of hyperfine fields in alloys became clear. The earlier model calculations of Daniel and Friedel [4] explained the negative hyperfine field of the early sp impurities. It was the works of Katayama and Co-workers [5-7] that exposed the understanding of the systematic trends of the hyperfine fields of sp impurities. These authors made the clarification that hybridization of the impurity s with the host d orbitals leads to bonding and anti bonding peaks for both spin up and spin down directions. They further explained that the intensities as well as positions of these peaks directly determine the hyperfine fields.

While sp impurities are non magnetic 3d and 4d impurities have a local moment in ferromagnets – a condition that complicates the situation more. The contribution to the hyperfine field is transferred by hybridization from the

polarized neighbouring d electrons ("transferred" hyperfine field). This is augmented by a "local" contribution due to the polarization of the local core and valence s electrons by the local d shell. This requires a self-consistent treatment of the electronic structure problem. Since core relaxations have to be taken into account due to the importance of the core polarization an "all electron" calculation has to be performed. The works of Janak [8] for the pure metals Fe, Co, and Ni on bond structure calculations were based on the local density approximation and recorded remarkable success expect that the hyperfine field for Fe was off the correct value by 25%. This success generated some surprise in view of the work of wilk and Vosko [9] whose conclusion on the basis of atomic calculations stressed that it would not be possible to calculate the hyperfine fields of local moment system by the local-density approximation prescribing that more serious treatment of the intra – atomic exchange was required.

In the latest work of Akai, Akai and kanamori [10-11] they performed self-consistent calculation for 3d and 4d impurities in Fe. They adopted the Korringa – Kohn – Rostoker (KKR) Green's function method for point defect calculations, Podlocky et al [12] and the Fe potential was calculated self – consistently. Leonard and Stefanou [13] have made similar calculations.

The first self – consistent calculation for 3d and 4d impurities in Ni were performed by Zeller [14]. These calculations have been extented to include potential perturbations on the neighbouring sites. Zeller [15] (unpublished) has given a detailed account of the calculations especially for the impurity moments and perturbed moments on the neighbouring sites. In parallel with the work of Akai et al, [11] for Fe, Bluge [16] carried out calculations of the hyperfine fields for 3d and 4d impurities in Ni.

This paper is a refinement of the calculation of hyperfine fields for 3d nd 4d impurities in Ni using KKR – CPA formalism in the framework of ensity functional theory. Since both the impurity potential as well as the otential of the neighbouring atoms are determined self-consistently we can calculate the hyperfine fields of both the impurity and the nearest neighbours. Also we shall estimate the scalar relativistic corrections to the hyperfine fields in the relativistic approximation, in which the orbtal contribution in neglected.

2 THEORETICAL METHODS

We base our calculations on density – functional theory (DFT) in the LSD). Several different forms for the local exchange correlation energy are used: In our calculations we used the LSD form given by Von Barth and Hedin [17] with the parameterization as modified by Moruzzi, Janak, and Williams [18] and the work of Vosko, Wilk and Nusair [19] fitted to the results of many – body calculations for the homogeneous electron gas by Monte Carlo Methods [20]. For the solution of DFT one – particle equations we adopt the multiple scattering theory, i.e. the Korringa-Kohn – Rostocker Green's function (KKR – GF) method for dilute impurity limit and the Korringa – Kohn – Rostocker Coherent – potential approximation (KKR – CPA) for concentrated alloys.

2.1 KKR – GF Method

The focus of spin – density – functional theory is centered on the electronic charge density n(r) and the magnetization density m(r). They are connected to the spin densities for majority spin up ↑ (+) and minority spin down ↓ (-) electrons by $n(r) = n_+(r) + n_-(r)$ and $m(r) = n_+(r) - n_-(r)$. The spin densities are determined from the one particle Green's function $G \pm (r,r', E)$ with the expression.

$$n+(r) = \Sigma\left|\Phi_r \pm(r)\right|^2 - \frac{1}{\pi}\int^{E_F} E_{bot}\, \mathrm{Im}\, G \pm (r,r^1, E)dE \qquad (1)$$

by energy integration from the bottom E_{bot} of the valence band up to the Femi level E_F. In a cell – centered representation the angular – momentum expansion for the Green's function can be written as in Zeller [21]

$$G_s^n \pm (r+R^n, r^1+R^{n^1}, E) + \sum_{LL'} R_L^n \pm (r,E) G_{LL'}^{nn^1} \pm (E) R_{L'}^{n^1} \pm (r^1, E) \qquad (2)$$

where we restrict the vector r and r^1 to the Wigner – Seitz cells around the atomic positions R^n and R^{n1}. The first term of equation (2) $G_s \pm$ represents the Green's function for the spin – dependent single-cell potential $V^n \pm (r)$ which is zero outside he Wigner Seitz cell Ω_n around the position R^n. This term is related to the free-space Green's function $g(r,r^1,E) = -(1/4\pi)\exp(i\sqrt{E}|r-r'|)/|r-r'|$ by an integral equation [21] with the integral restricted to cell Ω_n. In the second term of equation (2) we have the back – scattering contribution containing the structural Green's function matrix $G_{LL'}^{nn'} \pm (E)$ which is related to its free – space counterpart $g_{LL'}^{nn'}(E)$ by an algebraic Dyson equation.

$$G_{LL'}^{nn'} \pm (E) = g_{LL''}^{nn''}(E) \sum_{n'' L'' L''} g_{LL''}^{nn''}(E) t^{n''}{}_{L''L''} \pm (E) G_{L''',L'}^{n''n''} \pm (E) \qquad (3)$$

where we define the t matrices as

$$t^n_{LL'} \pm (E) = \int_{\Omega n} J_L g(r,E)\, V^n \pm (r) R^n_{L'} \pm (r,E)\, dr \qquad \text{.....(4)}$$

where J_L denote products of spherical Bassel functions and spherical harmonics, (21). We can calculate the single – cell wave function $R^n{}_L \pm (r,E)$ from the integral equation

$$R^n_L \pm (r,E) = J_L(r,E) + \int_{\Omega_n} g(r,r^I,E)\, V^n \pm (r^1)\, R^n_L \pm (r^I,E)\, dr^I \qquad \text{.....(5)}$$

The Dyson equation of (3) is solved in two steps by the intermediate use of the Green's function $G^0 \pm$ for the ideal periodic crystal. The Dyson equation which connects $G\pm$ and g can be solved by Fourier tranfrmation or alternatively by calculating the imaginary part of $G\pm$ similarly to density – of – states integrals and the real pat by a Kramers – Kroning integration [22] . The remaining Dyson equation, with $g^{nn}{}_{LL'}(E)$ replaced by $G_{LL'}^{nn'} \pm$ and with the t matrices $t^n{}_{LL'} \pm$ (E) replaced by their changes $\Delta t^n{}_{LL'} \pm (E)$ (E) with respect to the ideal crystal,

$$G_{LL'}^{nn'} \pm (E) = G^{onn'}{}_{LL'} \pm (E) + \sum_{n''L''L'''} G^{0nn'}{}_{LL''} \pm (E) \Delta t^{n''n'}{}_{L''L'''} \pm (E) G^{n''n'}{}_{L'''L''} \pm (E) \quad (6)$$

requires to solve a system of linear equation of finite dimensions determined by the number of perturbed atoms and angular momenta under consideration. We use angular momenta up to $l = 3$ and several shells of perturbed host potentials around the impurity site.

We enhance the efficiency of the KKR – GF method (1) by using group theory (ii) by transforming the integral in equation (1) along the real energy axis into a contour integral in the complex energy plane, where the green's function becomes smooth and structureless. Thus we carry out the integral with a small number of energy mesh points. For more details of this we refer to ref.[22]. The formulation in this section is not restricted to muffin – tin (MT) potentials but is valid for potentials of arbitrary shape.

1.1 K K R – CPA.

The above electronic structure by the corresponding Green's function within the KKR GF formalism is a very good beginning not only for impurity problems or dilute alloys, but also for concentrated ones. The principle behind more or less all alloys theories which has to be added to the KKR – GF formalism for that purpose, is to find a Green's function which represents the configuration average for the disordered alloy under consideration. If one restricts oneself to random alloys ignoring any correlation in the occupation of the various lattice sites, the best single-site theory at hand is the Coherent Potential Approximation (CPA) first suggested by Soven [23]. The hypothetical CPA medium representing the binary alloy $A_x B_{1-x}$ is found by the condition that the embedding of a A- or B- atom into this medium – weighted by the corresponding concentration x or 1-x, respectively should not cause any additional scattering. Conveniently we express this by means of the single site t – matrices t^α and the scattering path operators T^α (α = A,B,CPA):

$$\tau^{CPA}(E) = x\tau^{A}(E) + (1-x)\tau^{B}(E) \quad (7)$$

$$\tau^{CPA}(E) = \frac{1}{\Omega_{BZ}} X \int_{\Omega_{Bz}} d^3K \left[\left[t^{CPA}(E) \right]^{-1} - G(k,E) \right]^{-1} \quad (8)$$

$$\tau^{A(B)}(E) = \left[\left(t^{A(B)^{-1}} - (t^{CPA})^{-1} + (\tau^{CPA})^{-1} \right) \right]^{-1} \quad (9)$$

Here G(K,E) is the Founrier transform of the free-space Green's function. Since in Eqs. (7) – (9) only site – diagonal scattering – path operators occur, the site indices n,n'- and also the angular momentum indices L,L' as well as the spin indices - have been suppressed. The scattering operator $\mathcal{T}_{LL'}^{nn'}(E)$ Commonly used within the KKR – CPA formalism is linked to the KKR – Green's function $G_{LL'}^{nn'}(E)$ of the previous section by the relationship.

$$\tau = tGt + t \qquad (10)$$

Because of the various numerical problems in the solution of the KKR – CPA equations (7) – (9), this formalism could only be implemented 23 years ago by Stocks et al [24]. Since then very efficient computer codes have been developed making charge self-consistent calculations possible [25]. Also, corresponding relativistic [26] and spin – polarized relativistic [27] versions of the KKR – CPA formalism have been developed.

3. RESULTS AND DISCUSSIONS ON LOCAL MOMENTS, HYPERFINE FIELDS OF THE IMPURITIES, RELATIVISTIC AND NON – RELATIVISTIC EFFECTS.

3.1 LOCAL MOMENTS.

We present below the extensive results of the calculations for the local moments of the impurities and their nearest neighbours (NN). Our aim in this effort is to x-ray the numerical precision of the calculational procedures together with possible systematic errors involved in the exchange correlation approximations. By integrating the calculated spin densities over the impurity, Wigner – Seitz Spheres and by integrating the LDOS up to the Femi level we obtain the local Impurity moments as shown in Fig. 1 and 2. The moments arise mainly from polarization of d states whereas s, p and f polarizations add only a small negative contribution . (See table 1 of ref 22), Generally the calculated moments for the 4d impurities are much smaller than the ones for the 3d impurities. Agreement between theory is good for both 3d and 4d impurities except for Rh.

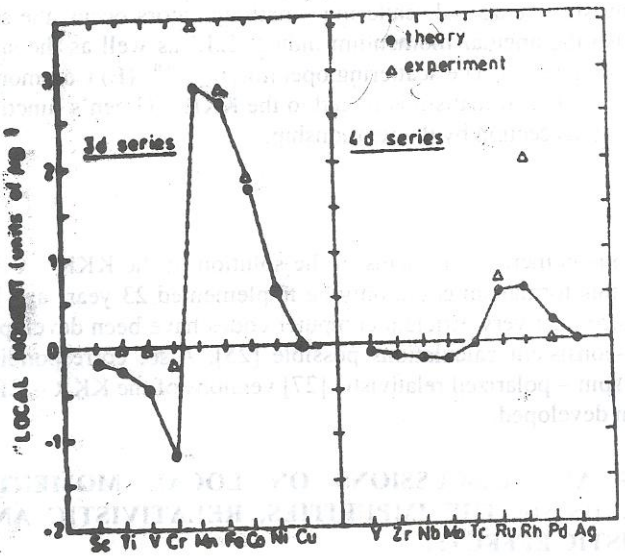

Fig. 1 Calculated local moments for 3d impurities and 4d impurities in Ni. The calculations refer to the semirelativistic approximation with VWN exchange correlation. The triangles denote experimental value

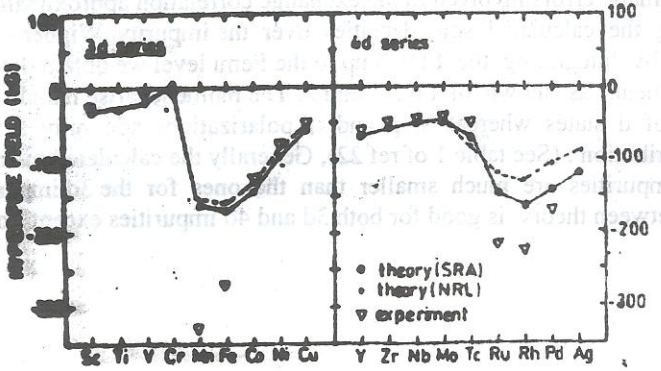

Fig. 2 Calculated hyperfine fields for 3d and 4d impurities in Ni. The large dots refer to the semirelativistic approximation the small ones to the nonrelativistic calculation. The experimental values are taken from a recent data collection [Ref2]

Our program for impurity calculation is different from the one used by Zeller. [22] Our program is based on the embedding philosophy discussed in section 2 so that the total charge density $\rho(r)$ is recalculated. Explicitly, core relaxations are allowed. We employ Wigner Seitz potentials from the 1s atoms in the cluster including relativistic effects in the semi relativistic approximation. For purposes of comparision, three different exchange correlation (XC) potentials are used namely: Von Barth and Hedin [17] (VBH), Vosko, Wilk, and Nusair (VWN) and Moruzzi, Janak and Williams [18] (MJW.) In table 1, we display the calculated moments for 3d impurities in NI.
The local moments are defined as the total magnetization within the local Wigner-Seitz sphere. The results for the above three exchange potentials (XC) calculated both non relativistically (NRL) and Semi relativistically (SRA) are given. When we compare the NRL results and the MJW exchange with the work of Zeller [21]

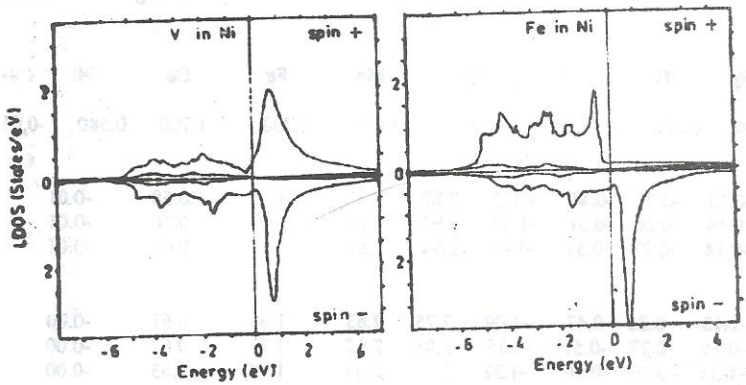

Fig. 3 Local density of states for V and Fe impurities in Ni. Two curves are shown for each spin direction. One gives the sum of s, p and f character, the other the total sum including the d character. The energies are given relative to the Fermi level

we observe that both yield identical results except for Cr. And Mn where there are appreciable differences. We shall comment on this later. The moment values for different exchange correlation potentials are scattered. This creates an impression of some errors involved in the exchange correlation approximation. The results for 3d impurities in table 1 and the corresponding results for 4d impurities in table 2 show a clear trend . The VBH exchange always gives the smallest moments

and the MJW exchange always the largest ones while he VMN values are intermediate. We assert that these differentials are due to the polarization dependence of the exchange potentials used. One observes that for all densities the exchange splitting of the MJW potential is larger than the VBH one and that the VWN one is intermediate. Therefore the MJW potential shows a stronger tendency toward magnetism than the VWN one. Except for Cr, we observe the absolute magnitudes of the differences in Table 1 and 2 is very small and completely insignificant compared with typical experimental errors. These values except for Cr. are reliable. As expected, for 3d impurities relativistic effects are not important and may be ignored. In the same way for 4d impurities the changes are slightly larger but rather small so that we have only listed the relativistic results.

Table 1. Local moments of 3d impurities in Ni for different XC Potentials in the non relativistic (NRL) and scalar relativistic (SRA) approximations VBH is the result using von Barth – Hedin XC potential (Ref 17), MJW is the result using the Moruzzi –Janak – Williams XC potential (Ref 18), VWN is the result using the Vosko, Wilk-Nusair XC potential (Ref. 19) Z is the theoretical results of Zeller (Ref 21). The local moments are given in units of μ_B

Potential	Sc	Ti	V	Cr	Mn	Fe	Co	Ni	Cu
Z	-0.140	-0.280	-0.560	-1.69	3.020	2.700	1.700	0.580	-0.01
NRL VBH	-0.13	-0.25	-0.46	-1.17	2.82	2.62	1.68	0.58	-0.01
VWN	-0.14	-0.26	-0.51	-1.35	2.92	2.66	1.71	0.56	-0.01
MJW	-0.14	-0.27	-0.51	-1.41	2.94	2.67	1.71	0.61	-0.01
SRA VBH	-0.13	-0.25	-0.47	-1.09	2.75	2.63	1.69	0.61	-0.00
VWN	-0.14	-0.27	-0.51	-1.25	2.85	2.67	1.73	0.62	-0.00
MJW	-0.14	-0.26	-0.50	-1.32	2.86	2.69	1.74	0.63	-0.00

Table 2. Local Moments of 4d impurities in Ni (same caption as in Table 1.)

Potential	Y	ZR	Nb	Mo	Tc	Ru	Rh	Pd	Ag
Z	-0.08	-0.14	-0.21	-0.24	-0.03	0.66	0.57	0.20	-0.01
SRA VBH	0.09	-0.13	-0.19	-0.22	-0.05	0.53	0.55	0.23	-0.00
VWN	-0.08	-0.14	-0.20	-0.23	0.05	0.55	0.56	0.23	-0.00
MJW	-0.08	-0.14	-0.20	-0.23	-0.05	0.56	0.56	0.24	-0.00

Let us examine why our calculations for Cr yield so widely different results.

While Co, Fe, and Mn. Couple ferromagnetically to the Ni host moment, Cr, V, Ti and S have an antiparallel moment. Calculation

with noninteger nuclear charges z indicate that there is a considerable range of z values for which both a ferromagnetic and anti-ferromagnetic solution disappears, e.g for Mn. When we move from Mn to Cr, the ferromagnetic solution becomes instable, whereas when we progress from Mn to Fe the anti ferromagnetic solution disappears. Thus both for Cr and Mn one is close to instabilities and any small change in the numerical procedures or in the Xc potential can lead to large differences. The physical interpretation is that the large differential is due to the fact that at the instability he susceptibilities of the system diverge. This is a severe problem for Cr, where the calculated values range from -1.08 to $-1.69\mu_B$. In the case of Mn, the problem also exists, however with a considerably smaller un-certainty. In the rest of the cases investigated our calculations are reliable.

In table 3, we list the changes of the moment on a neighbouring host atom. The moment is only slightly changed when the impurity moment aligns to the host moments but strongly decreases for the anti-parallel configuration.

Table 3. Change of moment of a nearest neighbour Ni atom (same nomenclature as Table 1)

	Impurity								
Potential	Sc	Ti	V	Cr	Mn	Fe	Co	Ni	Cu-
SRA VBH	-0.152	-0.191	-0.202	-0.192	-0.031	-0.01	+0.01	-0.00	-0.03
VWN	-0.152	-0.191	-0.202	-0.192	-0.031	-0.01	+0.00	0.00	-0.03
MJW	-0.152	-0.192	-0.202	-0.192	-0.031	-0.01	+0.00	0.00	-0.03

	Impurity							
Potential	Y	Zr	Nb	Mo	Tc	Ru	Rh	Pd	Ag
SRA VBH	-0.182	-0.231	-0.251	-0.271	-0.231	0.072	-0.011	0.011	-0.042

We observe in table 3 that these changes are very insensitive to the type of Xc potential used in the calculation.

3.1 LDOS.

In this section we present the local densities of states (L DOS). Within the impurity cell Ωn, the LDOS are easily calculated from the Green's function as

$$n\pm(E) = \frac{1}{\pi}\int_{\Omega_n} \mathrm{Im}\, G_{\pm}(r,r,E)dr \qquad (11)$$

We shall illustrate with the LDOS of V and Fe impurities in Ni. Fig 3, where for convenience of calculation we have replaced the integration volume by a sphere of equal volume. Detailed discussions of all 3d and 4d impurities in Ni are given in Ref. [22,28] . The majority – spin LDOS for the early 3d impurities Sc to Cr in Ni are always

characterized by Lorentzian – type virtual bound states (VBS) above the host d bands, as shown for V impurities in Fig 3.These VBS arise from the hybridization of atomic – like 3d levels of the impurities with the host conduction electrons of s and p character. As the atomic number increases from Sc to Cr, the VBS move towards the Femi level and become narrower. The behaviour of the minority – spin LDOS for the early impurities in Ni is similar to the one of the majority spin LDOS.

A significant feature of the majority spin LDOS of Fe and Co impurities in Ni is the small change both in shape and magnitude of the impurity LDOS compared to the host LDOS of pure Ni. The LDOS for Fe in Ni, shown in Fig 3 is similar to the one of pure Ni [18,22]. We affirm that the majority – spin electrons in Ni are nearly unperturbed by Fe and Co impurities leading to the very low residual resistivities of these impurities in Ni.

The minority – spin LDOS for Fe and Co in Ni show developed VBS above E_F , but also a considerable amount of states below E_F in the energy range of the host d bands.It is pertinent to note that the late transition – metal impurities have local moments being parallel to the host moment whereas the moments of the early transition – metal impurities as antiparallel to the host moments. It was Friedel [29,30] who first explained that the transition from ferromagnetic to anti-ferromagnetic coupling occurs, when the virtual bound state in the majority band crosses the Femi level, since then five majority d – states become unoccupied. Thus locally more minority states are occupied to achieve charge neutrality and in consequence the impurity moments are aligned oppositely to the host moments. The transition from this antiferromagnetism to ferromagnetism occurs nearly at the atomic number Z = 25 i.e at Mn impurities. This explains why calculations for Mn impurities is sensitive to numerical approximations. Furthermore the results depend on whether angular momenta up to l = 2 or 3 are used and on the particular form of the LSD approximation. (See Ref [28]).

3.2 HYPERFINE FIELDS OF THE IMPURITIES

A comprehensive review of the calculation of hyperfine interactions in metals can be found in ref. [31]. If we neglect the spin orbit interaction, the hyperfine field for impurities with cubic symmetry is given by the Femi contact term

$$H_{hf} = \frac{8}{3}\pi\mu_B m(o) \qquad (12)$$

where m(0) denotes the magnetization at the nuclear position. This is only valid for the non-relativistic case.

As shown in ref. [32] the correct formula for relativistic contact interaction filed is given by

$$H_{hf} = \frac{8}{3}\pi\mu_B m_T \qquad (13)$$

Where m_T means the average of the relativistic contact magnetization over the Thomson radius $r_T = \frac{Ze^2}{Mc^2}$

Table 4 Hyperfine fields of 3d impurities in Ni. Listed are the calculated hyperfine fields in the non-relativistic (NRL) and semi-relativistic approximation using the VWN xc potential. H^c_{hf} is the core contribution, H^v_{hf} the valence one, and $H^t_{hf} = H^c_{hf} + H^v_{hf}$ the total value. The experimental values $H^{expt.}_{hf}$ are from Krane (Ref. 3). All data are in KG.

Hyperfine field	Impurity Sc	T	V	Cr	Mn	Fe	Co	Ni	Cu
NRL H^c_{hf}	13	24.6	45	123 -	278	-261	-172	-65	-3.5
H^v_{hf}	- 41	- 47.6	- 61	- 111	124		104	40	21 - 48.5
H^t_{hf}	- 28	- 23.0	- 16	- 12	- 154	- 157	- 132	- 84	- 52
SRA H^C_{hf}	13.1	26	48	122	- 292	- 283	- 192	- 74	- 4.5
H^v_{hf}	- 44.2	- 53	- 68	- 117	131	114	49	- 21	- 55.5
H^t_{hf}	- 31.1	- 27	- 20	5	- 161	- 169	- 143	- 95	60
H^{expt}_{hf}	- 26	- 7.0	- 3.0	- 328	- 270	- 121	- 76	- 47	

Table 5 Hyperfine fields of 4d impurities in Ni (same nomenclature as in table 4)

Hyperfine Fields	Y	Zr	Nb	Mo	Tc	Ru	Rh	Pd	Ag
NRL H^C_{hf}	18	27	36	38	1	- 101	- 89	- 34	- 2
H^v_{hf}	- 72	- 73	- 74	- 74	- 58	- 22	- 42	- 74	- 88
H^t_{hf}	- 54	- 46	- 38	- 36	- 57	- 123	- 131	- 108	- 90
SRA H^C_{hf}	19	32	44	47	7	- 123	- 127	- 57	- 8
H^v_{hf}	- 89	- 90	- 94	- 95	- 78	- 24	- 39	- 86	- 113
H^t_{hf}	- 70	- 58	- 50	- 48	- 71	- 147	- 166	- 143	- 121
H^{expt}_{hf}	- 57	- 47.	- 41	- 40	- 48	- 217	- 225	- 170	- 122

In table 4 we display the calculated hyperfine fields of 3d impurities in Ni listing both the non relativistic (NRL) and the relativistic results (SRA) . In table 5 we give the corresponding results for 4d impurities. We used the VWN exchange correlation potential. In figs. 2a and 2b we compare the calculated and experimental data. There are strong negative values for the ferro-magnetically aligned impurities (Co, Fe, Mn and Pd, Rh, Ru) and moderately negative values for the impurities with negative local moments (Sc, Ti, V, Cr and Y. Zr, Nb, Mn, Tc). For both 3d and 4d, the values for the anti ferromagnetic impurities agree Well with the experiments, however, there are serious disagreements for the ferromagnetic impurities. In particular, the calculated values for Mn, and Fe the impurities with the largest moments are far too small. In the 4d serious we observe that the values for Rh and Ru are also too small. In general we observe that in the 3d series the relativistic corrections are rather small, typically about 10% for the ferromagnetic impurities. On the other hand for the 4d series, the corrections are rather important. For Rh, Pd, and Ag they are as large as 30%.

We observe that whereas the results for the impurities with a negative moment agree very well with experiments. The reverse is the case for the ferromagnetically aligned impurities. In particular the values for Fe and Mn are to small. The disagreement is not due to errors of the local moments, which we are well in agreement with neutron scattering data. Also the disagreement is not due to the neglect of orbital contributions which would give a positive contribution thus enhancing the discrepancy. It is our firm belief that this is due to an error of the local density approximation in calculating the magnetization close to the nucleus. We have earlier given the correct formula for this calculation.

4. SUMMARY AND CONCLUSION

We have performed, in detail, self-consistent calculations for the hyperfine Fields of transition metal impurities in Ni using new improved formulas for the relativistic generalizations of the contact orbital and dipolar contributions to the hyperfine fields. For the relativistic contact interaction the spin density near the nucleus has to be averaged over a region whose diameter is the Thomson radius. For transition metal impurities the core polarization induced by sd exchange leads to a large core hyperfine field and is negative and proportional to the local moment . Additionally an important valence hyperfine field consisting of a transferred and a local contribution is obtained. The transferred field is negative for transition metal impurities and arises form the hybridization with the spin

polarized d electons of the Ni neighbours. This was explained by Katayama et al [5-7]. The results indicate that the local valence field is directly proportional to the local moment and is positive contrary to the core field. This is caused by the enhanced population of the majority s – states.

The calculations reproduce the experimental values of the hyperfine fields for large moment cases (eg Fe) there are serious large discrepancies and we attribute these to failures of the local density approximations in describing the core polarization. This will be the focus of our next research.

ACKNOWLEDGEMENT

I wish to thank Prof. H. Akai of Osaka University Japan for supplying me the KKR-CPA code used in the computation. The invaluable of help of Acotech Computers University of Port Harcourt is here acknowledged.

REFERENCES

[1] S. Blugel, H. Akai, R. Zeller, P.H. Dederichs, Phys. Rev. B. 35 (1987) 3271.

[2] G.N. Rao, Herperfine Interact. 7, 141, (1979)

[3] K.S. Krane, Herperfine Interact. 16, 1069 (1983).

[4] E. Daniel and J. Friedel, J. Phys. Chem. Solids 24, 1601 (1963).

[5] H. Katayama, K Terakura and J. Kanamori Solid State Commun. 29, 431 (1979).

[6] H – Katayama – Yoshida, K Terakura and J. Kanamori J. Phys. Soc. Jpn, 46,822, (1979) 48, 1504 (1980), 49, 972 (1980).

[7] J. Kanamri, H. Katayama – Yshida and K. Terakura, Hyperfine Interact 8, 573 (1981).

[8] J.F. Janak Phys. Rev. B.20, 2206 (1979)

[9] L. Wilk and S. H. Vosko, Phys. Rev. A15, 1839 (1977)

[10] M. Akai, H.Akai, and J. Kanamori J. Phys. Soc. Jpn. 54, 4257 (1985)

[11] H. Akai, M. Akai and J. Kanamori J. Phys. Soc. Jpn 54, 4257 (1985).

[12] R. Podioucky, R. Zeller, and P.H.Dederichs Phys. Rev. B. 22, 5777 (1980.

[13] P. Leonard and N. Stefanou, Phylos. Mag. B 51, 151 . (1985).

[14] R. Zeller; in Physics of Transition Metals 1980, 10p Conf. Ser No. 55 edited by P. Rhodes (IOP, London, 1981) p.265.

[15] R. Zeller (unpublished) .

[16] S. Blugel, Diplomarbeit, Technische Hoschschu le, Aachen, 1983.

[17] U. Von Barth and L. Hedin J. Phys C5 (1972) 1629.

[18] V.L. Moruzzi, J.F. Janak and A.R. Williams . Calculated Electronic Properties o f Metals (Pergamon Press, new York 1978)

[19] S.H. Vosko, L. Wilk and M. Nusair, Can J. Phys 58 (1980) 1200.

[20] D.M. Ceperley and B.J. Alder. Phys. Rev. Lett 45,566 (1980)

[21] R. Zeller J. Phys. C. 20 (1987) 2347.

[22] R. Zeller J. Phys. F. 17 (1987) 2123.

[23] P. Soven, Phys. Rev. 156 (1967) 809.

[24] G.M. Stocks, W.M. Termerman and B.L Gyrffy Phys. Rev. Lett. 41 (1978) 339.

[25] H. Akai J. Phys. Soc. Jpn 51 (1952) 1176. H. Winter and G.M Stocks Phys. Rev. B27 (1983) 882 H. Akai J. Phys. Condens Matter 1 (1989) 8045.

[26] J.B. Staunton, B.L. Gyorffy and P. Weinberger J. Phys. F 10, (1980) 2665.
[27] H. Ebert, B. Drittler and H. Akai unpublished.

[28] B. Drittler, N. Stefanou, S. Blugel, R. Zeller and P.H. Dederichs Phys. Rev. B. 40(1989) 8203.

[29] J. Friedel, Nuovo Cimento 10 suppl. No. 2 (1958) 287.

[30] I.A. Campbell and A.A. Gomes Proc. Phys. Soc. London 91 (1967) 319.

[31] H. Akai, M.Akai, S. Bludgel, B. Drittler, H. Ebert, K. Terakura, R. Zeller and P.H. Dederichs Prog. Theor. Phys. Suppl. 101 (1990). 11.

[32] S. Blugel, H. Akai, R. Zeller and P.H. Dederichs Phys. Rev. B. 35 (1987) 3271.